Control experiments with fluoride ion and each solvent have been carried out alongside the carborane experiments in order to assess potential problems of fluoride ion interaction with the solvent prior to carborane attack. It is to be noted, however, that preliminary studies with acetonitrile and tetrahydrofuran show no attack of solvent by fluoride ion under the conditions of the fluoride ion/carborane studies involving 1,6-$C_2B_4H_6$, 2,4-$C_2B_5H_7$, or the 1,2- and 1,7-isomers of $C_2B_{10}H_{12}$.[20]

As mentioned above, attack of dialkylamide anion (in acetonitrile) on *closo*-2,4-$C_2B_5H_7$ also gives rise to *nido*-2,4-$C_2B_4H_7^-$ and along the way produces two intermediates, in which at least one is thought to represent progressive cage opening of the seven-atom cage system.[4] Thus far, we have not noticed intermediates during the fluoride ion/2,4-$C_2B_5H_7$ reaction or in the other fluoride/carborane reactions described in this report.

(20) See the reference in footnote 18 for comments about the reactivity, or inertness, of fluoride ion with acetonitrile.

In closing, fluoride ion appears to be unique among the halides in that the higher halide ions do not appear to give cage-opened products by starting with the above *closo*-carboranes.[21]

Acknowledgment. We wish to thank the National Science Foundation, Grants CHE-8617068 and CHE-8922339, and the MBRS-NIH program for partial support of this study. We also thank California State University, Sacramento, CA, for access to the multiflow trace (NSF Grant CHE-8822716) minisupercomputer facilities and San Diego State University for access to the San Diego Supercomputer Regional Facility. The NMR data were obtained by the use of a Bruker AM-400 instrument at CSULA, funded by NIH Grant RR-08101-13S1, by NSF Grant DMB-8503839, and by the Keck and Dreyfus Foundations.

(21) It has come to our attention that others have noticed the action of fluoride ion on derivatives of 1,2-$C_2B_{10}H_{12}$, and results similar to those reported herein for the parent *o*-carborane were observed: Varadrajan, A.; Gomez, F.; Hawthorne, M. F. Unpublished studies.

Contribution from the Department of Chemistry, University of Wyoming, Laramie, Wyoming 82071, and Chemistry Laboratory I, Inorganic Chemistry, H. C. Ørsted Institute, Universitetsparken 5, DK-2100 Copenhagen Ø, Denmark

Tetranuclear Heterometallic Complexes of the General Types $[M\{(OH)_2CrA_4\}_3]^{5+}$ and $[M\{(OH)_2CoA_4\}_3]^{5+}$

Derek J. Hodgson,*[1a] Kirsten Michelsen,*[1b] Erik Pedersen,*[1b] and Debra K. Towle[1c]

Received July 12, 1990

Series of tetranuclear heteronuclear complex ions of the general types $[M\{(OH)_2CrA_4\}_3]^{5+}$ and $[M\{(OH)_2CoA_4\}_3]^{5+}$, where M is a divalent metal ion and A_4 is a single tetradentate amine ligand, two bidentate amines, or four monodentate amines, have been synthesized and characterized. The structure of the cobalt(II)/chromium(III) complex $[Co\{(OH)_2Cr(bispictn)\}_3](ClO_4)_5 \cdot 6H_2O$ (where bispictn is *N,N'*-bis(2-pyridylmethyl)-1,3-propanediamine, $C_{15}H_{20}N_4$) has been determined by single-crystal X-ray diffraction techniques. The complex crystallizes in the acentric space group $P31c$ of the trigonal system with two tetranuclear species in a cell of dimensions a = 16.144 (5) Å and c = 15.091 (2) Å. The structure has been refined to a value of the weighted R factor of 0.046 based on 1604 independent observed reflections. The Co atom lies on the 3-fold axis and is surrounded by six bridging hydroxo groups. Hence, the complex can be viewed as consisting of three *cis*-$[Cr(bispictn)(OH)_2]^+$ units, which act as bidentate ligands to the central cobalt(II) core. The Co–O bond lengths are 2.050 (5) and 2.166 (5) Å, while the Cr–O distances are 1.902 (5) and 1.921 (5) Å. The Co–Cr distance in the tetramer is 3.064 (2) Å, comparable to the values in bis(μ-hydroxo)dichromium(III) dimers. The magnetic properties of the complexes have been investigated and are compared with the theoretical values obtained by fitting to the appropriate Hamiltonian. General energy diagrams illustrating the relation among energy, spin, and degeneracy for tetranuclear systems having S_1 between $^1/_2$ and $^5/_2$, $S_2 = S_3 = S_4 = {}^3/_2$, $J_{12} = J_{13} = J_{14} = J$, and $J_{23} = J_{34} = J_{42} = 0$ are given; these diagrams illustrate that in all cases, independent of S_1 and the sign of J, the ground state has a higher spin than the nearest excited states. This has important consequences for the variation of the effective magnetic moments with the temperature.

Introduction

During the past few years we[2-4] and others[5] have been interested in the development of polynuclear transition-metal ions formed from the interaction of 2 or more mol of *cis*-$[CrA_4(OH)_2]^+$ (where A_4 is a single tetradentate amine ligand, two bidentate amines, or four monodentate amines), or its cobalt(III) analogue, with metal halides. The resultant heteronuclear or homonuclear complex ion can be viewed as stemming from the interaction of the bidentate *ligand* $[CrA_4(OH)_2]^+$ with the central metal ion, and complexes with two, three, and four such ligands coordinated to a single metal have been isolated, characterized, and briefly described.[2-5] We have now undertaken a complete synthetic and physical study of the tetranuclear complexes of this type and have demonstrated the amazing versatility of our approach for the formation of tetranuclear species; virtually any central metal ion, M, can be coordinated to three bidentate $[CrA_4(OH)_2]^+$ moieties to form the complex.

We report here the synthetic approach, the magnetic and EPR properties, and the structures of this new series of tetranuclear heterometallic complexes.

Experimental Section

Syntheses. The following complexes were prepared according to procedures described in the literature: *N,N'*-bis(2-pyridylmethyl)-1,3-propanediamine (bispictn),[6] *cis*-β-$[Co(bispictn)Cl_2]Cl \cdot 0.5HCl$,[7] *cis*-$[Cr(NH_3)_4(OH)(H_2O)]S_2O_6 \cdot H_2O$,[8] and *cis*-$[Co(NH_3)_4(H_2O)_2]Br_3$.[9] *cis*-$\beta$-$[Cr(bispictn)Cl_2]Cl \cdot 2H_2O$ and $[Cr(en)_2Cl_2]Cl$ were prepared from $CrCl_3$ and the appropriate amine in DMSO by following the method described for α-$[Cr(pico)_2Cl_2]Cl$.[10] The compounds were converted into the other starting materials as described below.

Starting Materials. 1. *cis*-β-$[Cr(bispictn)(OH)(H_2O)](ClO_4)_2 \cdot 2H_2O$. *cis*-$\beta$-$[Cr(bispictn)Cl_2]Cl \cdot 2H_2O$ (0.41 g, 0.91 mmol) was dissolved in water (3 mL) and a solution of sodium hydroxide (1 mL, 2 M). The solution was heated briefly (80 °C) and then filtered. After the solution was cooled on ice, sodium perchlorate (2 g) was added, and the solution

(1) (a) University of Wyoming. (b) H. C. Ørsted Institute. (c) Present address: E. I. du Pont de Nemours & Co., Edgemoor, DE 19809.
(2) Hodgson, D. J.; Michelsen, K.; Pedersen, E.; Towle, D. K. *J. Chem. Soc., Chem. Commun.* **1988**, 426-428.
(3) Hodgson, D. J.; Michelsen, K.; Pedersen, E. *J. Chem. Soc., Chem. Commun.* **1988**, 1558-1560.
(4) Corbin, K. M.; Hodgson, D. J.; Lynn, M. H.; Michelsen, K.; Nielsen, K. M.; Pedersen, E. *Inorg. Chim. Acta* **1989**, *159*, 129-131.
(5) Müller, S.; Thewalt, U. *Z. Naturforsch.* **1989**, *44B*, 257.
(6) Goodwin, H. A.; Lions, F. *J. Am. Chem. Soc.* **1962**, *82*, 5021.
(7) Gibson, J. G.; McKenzie, E. D. *J. Chem. Soc. A* **1971**, 1666.
(8) Springborg, J.; Schaeffer, C. *Inorg. Synth.* **1978**, *18*, 80.
(9) Jørgensen, S. M. *Z. Anorg. Chem.* **1892**, *2*, 294.
(10) Michelsen, K. *Acta Chem. Scand.* **1972**, *26*, 1517.

0020-1669/91/1330-0815$02.50/0

Table I. Analytical Data for New Complexes with bispictn, $C_{15}H_{20}N_4$

no.	compd	anal.: found, % (calcd, %) M(II)	M(III)	C	H	N	Cl	yield, %
4a	$[Mn\{(OH)_2Cr(C_{15}H_{20}N_4)\}_3](ClO_4)_5\cdot 6H_2O$	3.24 (3.26)	9.28 (9.24)	32.15 (32.03)	4.33 (4.66)	9.99 (9.96)	10.71 (10.51)	45
1a	$[Co\{(OH)_2Cr(C_{15}H_{20}N_4)\}_3](ClO_4)_5\cdot 6H_2O$	3.43 (3.48)	9.35 (9.22)	31.92 (31.96)	4.33 (4.64)	9.93 (9.94)	10.50 (10.48)	47
3a	$[Ni\{(OH)_2Cr(C_{15}H_{20}N_4)\}_3](ClO_4)_5\cdot 6H_2O$	3.50 (3.47)	9.20 (9.22)	31.97 (31.96)	4.23 (4.65)	9.89 (9.94)	10.60 (10.48)	45
2a	$[Zn\{(OH)_2Cr(C_{15}H_{20}N_4)\}_3](ClO_4)_5\cdot 6H_2O$	3.85 (3.85)	9.24 (9.19)	31.70 (31.84)	4.30 (4.63)	10.16 (9.90)	10.25 (10.44)	36
5a	$[Mg\{(OH)_2Cr(C_{15}H_{20}N_4)\}_3[ClO_4)_5\cdot 6H_2O$		9.68 (9.62)	33.34 (33.35)	4.41 (4.60)	10.45 (10.37)	10.81 (10.94)	35
4b	$[Mn\{(OH)_2Co(C_{15}H_{20}N_4)\}_3(ClO_4)_5\cdot 6H_2O$	3.22 (3.22)	10.33 (10.35)	31.57 (31.64)	4.20 (4.60)	9.77 (9.84)	10.57 (10.38)	73
1b	$[Co\{(OH)_2Co(C_{15}H_{20}N_4)\}_3](ClO_4)_5\cdot 6H_2O$	13.61[a] (13.77)		31.23 (31.57)	3.96 (4.59)	9.61 (9.82)	10.32 (10.35)	49
3b	$[Ni\{(OH)_2Co(C_{15}H_{20}N_4)\}_3](ClO_4)_5\cdot 6H_2O$	3.45 (3.43)	10.35 (10.43)	31.86 (31.57)	4.06 (4.59)	9.77 (9.82)	10.68 (10.35)	53
2b	$[Zn\{(OH)_2Co(C_{15}H_{20}N_4)\}_3](ClO_4)_5\cdot 6H_2O$	3.83 (3.80)	10.36 (10.29)	31.45 (31.44)	4.03 (4.57)	9.85 (9.78)	10.30 (10.31)	60
5b	$[Mg\{(OH)_2Co(C_{15}H_{20}N_4)\}_3](ClO_4)_5\cdot 6H_2O$		10.64 (10.77)	32.91 (32.93)	4.17 (4.54)	10.18 (10.24)	10.93 (10.80)	60

[a] Total amount of cobalt.

was acidified (pH ~ 6.5) with perchloric acid. The precipitate that formed immediately was filtered out and washed with ethanol (99%). Yield: 0.32 g (61%). Recrystallization from boiling water implied a loss of approximately 30%. Anal. Calcd for $[Cr(bispictn)(OH)(H_2O)](ClO_4)_2\cdot 2H_2O$: Cr, 8.99; C, 31.16; N, 9.69; H, 4.71; Cl, 12.26. Found: Cr, 9.04, C, 30.81; N, 9.75; H, 4.36; Cl, 12.37.

2. *cis*-β-[Co(bispictn)(OH)(H$_2$O)](ClO$_4$)$_2$·2H$_2$O. Powdered silver nitrate (1.2 g) was poured into a solution of sodium hydroxide (2 M, 3 mL), and the brown-black precipitate of silver oxide that separated was washed by decantation with water several times. Then *cis*-β-$[Co(bispictn)Cl_2]Cl\cdot{}^1/_2HCl\cdot 3H_2O$ (0.60 g ~ 1.21 mmol) was added. After being stirred for 5 min, the suspension was filtered. Sodium perchlorate (1 g) was added to the solution, which was cooled on ice and acidified (pH ~ 6.5) with perchloric acid. Scratching with a spatula initiated the formation of red crystals of the hydroxo aqua complex. The compound was washed with a solution of sodium perchlorate (1 M) and with ethanol (96%). Yield: 0.40 g (56%). Recrystallization from boiling water implied a loss of approximately 30%. Anal. Calcd for $[Co(bispictn)(OH)(H_2O)][(ClO_4)_2\cdot 2H_2O$: Co, 10.07; C, 30.79; N, 9.57; H, 4.64; Cl, 12.12. Found: Co, 10.12; C, 30.76; N, 9.62; H, 4.26; Cl, 12.10.

3. *cis*-[Cr(NH$_3$)$_4$(H$_2$O)$_2$]Br$_3$. *cis*-$[Cr(NH_3)_4(OH)(H_2O)]S_2O_6\cdot H_2O$ (1.20 g ~ 3.60 mmol) was dissolved in a dilute solution of hydrogen bromide (2.2 M, 2.2 mL) at 0 °C. Subsequently, a concentrated solution of hydrogen bromide (9 M, 4.5 mL) was added dropwise with cooling and stirring. The orange precipitate was filtered out and washed with ethanol (96%). Yield: 0.96 g (67%). Anal. Calcd for $[Cr(NH_3)_4(H_2O)_2]Br_3$: Cr, 13.13; Br, 60.55. Found: Cr, 13.11; Br, 60.64.

4. *cis*-[Cr(NH$_3$)$_4$(OH)(H$_2$O)](ClO$_4$)$_2$. *cis*-$[Cr(NH_3)_4(H_2O)_2]Br_3$ (0.60 g ~ 1.52 mmol) was dissolved in water (1 mL) at room temperature. Sodium perchlorate (1.5 g) and a solution of sodium hydroxide (2 M, 0.7–0.8 mL) were added with stirring and cooling on ice. After 15 min the red compound that separated was filtered out and washed with ethanol (96%). Yield: 0.50 g (93%). Anal. Calcd for $[Cr(NH_3)_4(OH)(H_2O)](ClO_4)_2$: Cr, 14.69; N, 15.82; H, 4.27; Cl, 20.02. Found: Cr, 14.65; N, 15.80; H, 4.22; Cl, 20.06.

5. *cis*-[Cr(en)$_2$(OH)(H$_2$O)](ClO$_4$)$_2$. *cis*-$[Cr(en)_2Cl_2]Cl$ (0.80 g ~ 2.88 mmol) was suspended in water (4 mL). A solution of sodium hydroxide (2 M, 2 mL) was added, and the suspension was heated for a few minutes (60–65 °C). After the mixture was filtered and the filtrate was cooled on ice, sodium perchlorate (2.5 g) was added with stirring, and the solution was acidified (pH ~ 6) with perchloric acid (4 M). The red compound was filtered out after 1 h and washed with ethanol. Yield: 0.64 g (55%). Anal. Calcd for $[Cr(C_2H_8N_2)_2(OH)(H_2O)](ClO_4)_2$: Cr, 12.80. Found: Cr, 12.74.

Stock Solutions. Solution A. Five solutions each containing 0.3 mmol of $[Cr(bispictn)(OH)_2]^+$ were prepared by the following procedure: $[Cr(bispictn)(OH)H_2O)](ClO_4)_2\cdot 2H_2O$ (174 mg ~ 0.3 mmol) was suspended in water (3 mL). A solution of sodium hydroxide (2 M, 3 drops, ~ 0.3 mmol) was added with stirring. After being filtered, the solution (solution A) was ready for use in the syntheses of compounds of the general type $[M\{(OH)_2Cr(bispictn)\}_3](ClO_4)_5\cdot 6H_2O$.

Solution B. Five solutions each containing 0.3 mmol of $[Co(bispictn)(OH)_2]^+$ were prepared exactly as in solution A but from $[Co(bispictn)(OH)(H_2O)](ClO_4)_2\cdot 2H_2O$ (176 mg ~ 0.3 mmol). The solutions (solution B) were used in the syntheses of the compounds $[M\{(OH)_2Co(bispictn)\}_3](ClO_4)_5\cdot 6H_2O$.

Solution C. Five solutions each containing 0.6 mmol of $[Cr(NH_3)_4(OH)_2]^+$ were prepared by the following procedure: $[Cr(NH_3)_4(OH)(H_2O)](ClO_4)_2$ (213 mg ~ 0.6 mmol) was suspended in water (1.5 mL). A solution of sodium hydroxide (2 M, 7 dr. ~ 0.6 mmol) was added with stirring. After being filtered, the solution (solution C) was ready for use in the syntheses of the compounds $[M\{(OH)_2Cr(NH_3)_4\}_3](ClO_4)_5\cdot XH_2O$.

Solution D. Three solutions each containing 0.6 mmol of $[Co(NH_3)_4(OH)_2]^+$ were prepared by the following procedure: $[Co(NH_3)_4(H_2O)_2]Br_3$ (242 mg ~ 0.6 mmol) was dissolved in water (1 mL). A solution of sodium hydroxide (2 M, 10 drops) was added, until the pH was approximately 8.5. After being filtered, the solution (solution D) was ready for use in the syntheses of the compounds $[M\{(OH)_2Co(NH_3)_4\}_3]Br_5\cdot YH_2O$.

Solution E. Three solutions each containing 0.6 mmol of $[Cr(en)_2(OH)_2]^+$ were prepared exactly as in solution C but from $[Cr(en)_2(OH)(H_2O)](ClO_4)_2$ (244 mg ~ 0.6 mmol). Each solution (solution E) was used in the synthesis of the compounds $[M\{(OH)_2Cr(en)_2\}_3](ClO_4)_5\cdot 3H_2O$.

Heteronuclear Compounds. A. [M{(OH)$_2$Cr(bispictn)}$_3$](ClO$_4$)$_5$·6H$_2$O (M = Co, Zn, Ni, Mn, Mg). Aqueous solutions (1 mL) of each of the compounds $CoCl_2\cdot 6H_2O$ (24 mg ~ 0.1 mmol), $Zn(NO_3)_2\cdot 6H_2O$ (30 mg ~ 0.1 mmol), $NiCl_2\cdot 6H_2O$ (24 mg ~ 0.1 mmol), $MnCl_2\cdot 4H_2O$ (20 mg ~ 0.1 mmol), and $MgSO_4\cdot 7H_2O$ (25 mg ~ 0.1 mmol) were added dropwise to five of the stock solutions A. The orange-red (Co, Ni, Mn) or red (Zn, Mg) crystals that separated were filtered out and washed with a solution of sodium perchlorate (1 M) and with ethanol (96%). Analytical data are summarized in Table I.

B. [M{(OH)$_2$Co(bispictn)}$_3$](ClO$_4$)$_5$·6H$_2$O (M = Co, Zn, Ni, Mn, Mg). The compounds were synthesized exactly as the corresponding chromium complexes but from stock solutions B. Analytical data are summarized in Table I.

C. [M{(OH)$_2$Co(NH$_3$)$_4$}$_3$](ClO$_4$)$_5$·XH$_2$O (M = Co, Zn, Ni, Mn, Mg). Each of the solid compounds $CoCl_2\cdot 6H_2O$ (48 mg ~ 0.2 mmol), $(NH_4)_2ZnCl_4$ (48 mg ~ 0.2 mg), $NiCl_2\cdot 6H_2O$ (48 mg ~ 0.2 mmol), $MnCl_2\cdot 4H_2O$ (40 mg ~ 0.2 mmol), and $MgCl_2\cdot 6H_2O$ (40 mg ~ 0.2 mmol) was added with shaking to five of the standard solutions C. The solutions were cooled on ice, and soon orange-red crystals started to separate. After 2 h the compounds were filtered out and washed as described above. Analytical data are summarized in Table II. The content of crystal water varies.

D. [M{(OH)$_2$Co(NH$_3$)$_4$}$_3$]Br$_5$·YH$_2$O (M = Co, Ni). The compounds were synthesized exactly as the corresponding chromium complexes but from stock solutions D. The red-brown (Co) and yellow-red (Ni) compounds were washed with ethanol (96%). Analytical data are summarized in Table II.

E. [M{(OH)$_2$Cr(en)$_2$}$_3$](ClO$_4$)$_5$·3H$_2$O (M = Co, Zn, Ni). The compounds were synthesized exactly as the corresponding compounds with ammonia but from stock solutions E. Analytical data are summarized in Table II.

Table II. Analytical Data for New Complexes with Ammonia and en, $C_2H_8N_2$

no.	compd	anal.: found, % (calcd, %) M(II)	M(III)	C	H	N	Cl/Br	yield, %
1c	$[Co\{(OH)_2Cr(NH_3)_4\}_3](ClO_4)_5\cdot 6H_2O$	5.37 (5.23)	13.95 (13.85)		4.34 (4.83)	14.90 (14.92)	15.83 (15.73)	25
2c	$[Zn\{(OH)_2Cr(NH_3)_4\}_3](ClO_4)_5\cdot 4H_2O$	6.40 (5.96)	14.17 (14.22)		4.38 (4.59)	15.36 (15.32)	15.95 (16.16)	26
3c	$[Ni\{(OH)_2Cr(NH_3)_4\}_3](ClO_4)_5\cdot 6H_2O$	5.22 (5.21)	13.78 (13.85)		4.23 (4.83)	15.06 (14.92)	16.90 (15.73)	60
4c	$[Mn\{(OH)_2Cr(NH_3)_4\}_3](ClO_4)_5\cdot 4H_2O$	5.41 (5.06)	14.50 (14.35)		4.21 (4.66)	15.32 (15.47)	16.78 (16.31)	27
5c	$[Mg\{(OH)_2Cr(NH_3)_4\}_3](ClO_4)_5\cdot 4H_2O$		14.75 (14.77)		3.95 (4.77)	16.08 (15.92)	18.70 (16.79)	15
1d	$[Co\{(OH)_2Co(NH_3)_4\}_3]Br_5\cdot 7H_2O$	21.98[a] (22.08)				15.82 (15.74)	37.27 (37.42)	30
3d	$[Ni\{(OH)_2Co(NH_3)_4\}_3]Br_5\cdot 10H_2O$		15.76 (15.76)			14.99 (14.99)	36.77 (35.62)	37
1e	$[Co\{(OH)_2Cr(C_2H_8N_2)_2\}_3](ClO_4)_5\cdot 3H_2O$	4.99 (4.80)	12.68 (12.69)	11.72 (11.73)	5.10 (4.92)	13.70 (13.68)	14.62 (14.43)	25
2e	$[Zn\{(OH)_2Cr(C_2H_8N_2)_2\}_3](ClO_4)_5\cdot 3H_2O$	5.71 (5.29)	12.65 (12.63)	11.78 (11.67)	4.91 (4.90)	13.89 (13.61)	14.77 (14.35)	18
3e	$[Ni\{(OH)_2Cr(C_2H_8N_2)_2\}_3](ClO_4)_5\cdot 3H_2O$	5.54 (4.78)	12.35 (12.70)	11.52 (11.73)	4.93 (4.92)	13.60 (13.68)	14.71 (14.43)	51

[a] Total amount of cobalt.

Table III. Crystallographic Data

$[CoCr_3C_{45}H_{66}N_{12}O_6](ClO_4)_5\cdot 6H_2O$	λ = 0.71073 Å
a = 16.144 (5) Å	ρ_{obsd} = 1.60 g cm^{-3};
c = 15.091 (2) Å	ρ_{calcd} = 1.60 g cm^{-3}
V = 3406 (4) Å^3	μ = 9.82 cm^{-1}
Z = 2	transm coeff = 0.80–1.00
fw 1691.4	$R(F_o)$ = 0.063
space group $P\bar{3}1c$ (No. 159)	$R_w(F_o)$ = 0.046
T = 22 °C	

Analyses. The metal analyses were performed on a Perkin-Elmer 403 atomic absorption spectrometer. The microanalytical laboratory of the H. C. Ørsted Institute carried out the carbon, nitrogen, hydrogen, and halogen analyses by standard methods.

Physical Measurements. Absorption spectra were recorded on a Cary Model 118 spectrophotometer. The spectra are characterized by their maxima (ϵ, λ), where the molar extinction coefficient ϵ is in units of l mol^{-1} cm^{-1} and λ is in nm. The compounds were dissolved in different organic solvents, selected so as to ensure the highest solubility. The diffuse reflectance spectra were obtained on a Perkin-Elmer Lambda 7 spectrophotometer. The magnetic susceptibilities of powdered samples were measured by the Faraday method in the temperature range 2–300 K at a field strength of 1.3 T. The magnetic field was calibrated with $Hg[Co(NCS)_4]$.[11] A more detailed description of the equipment is published elsewhere.[12,13] The X-ray powder photographs were obtained on a camera of the Guinier type with Cu Kα radiation. EPR spectra were recorded on a Bruker ESP-300 spectrometer equipped with an Oxford ESR-9 gas-flow cryostat.

X-ray Data Collection and Reduction. The structure of a sample complex, $[Co\{(OH)_2Cr(bispictn)\}_3](ClO_4)_5\cdot 6H_2O$, was solved. An orange hexagonal prismatic crystal was mounted on an Enraf-Nonius CAD4 diffractometer equipped with Zr-filtered Mo radiation [$\lambda(K\alpha_1)$ = 0.70926 Å]. Preliminary examination suggested that the crystals belonged to either the trigonal or hexagonal classes, and examination of the intensities of several sets of carefully chosen reflections demonstrated that the symmetry is indeed trigonal; systematic absences of $l = 2n + 1$ for hhl data are consistent with the space groups $P\bar{3}1c$ (No. 163) or $P\bar{3}1c$ (No. 159). With two tetranuclear molecules in the unit cell, the cobalt centers would be constrained to either 32 (D_3) or $\bar{3}$ (S_6) symmetry in $P\bar{3}1c$, while the chromium centers would have 2 (C_2) or $\bar{1}$ (C_i) symmetry. In principle, 32 symmetry at cobalt is possible for a complex of this type, while $\bar{3}$ symmetry is not. Inversion at chromium is not possible in this complex, of course, and rotation symmetry at chromium is impossible in the β form of the complex. In $P\bar{3}1c$, however, cobalt is constrained only to 3 (C_3) symmetry and the Cr centers are unconstrained. Hence, the space group was deduced to be $P\bar{3}1c$, and this assignment was confirmed by the eventual structure refinement.

Table IV. Positional Parameters for $[Co\{(OH)_2Cr(bispictn)\}_3](ClO_4)_5\cdot 6H_2O$

atom	x	y	z
Co	0.3333	0.6667	0.6000
Cr	0.28698 (9)	0.45865 (8)	0.6170 (1)
Cl(1)	0.6667	0.3333	0.4080 (3)
Cl(2)	0.0000	0.0000	0.2285 (3)
Cl(3)	0.1742 (2)	0.4399 (2)	0.2845 (2)
O(1)	0.2688 (3)	0.5378 (3)	0.5352 (4)
O(2)	0.3636 (3)	0.5748 (3)	0.6819 (3)
O(11)	0.6667	0.3333	0.5009 (8)
O(12)	0.5860 (5)	0.3343 (6)	0.3772 (6)
O(21)	0.0000	0.0000	0.3091 (16)
O(22)	−0.0608 (11)	−0.0875 (9)	0.2033 (11)
O(31)	0.2256 (6)	0.4665 (7)	0.2045 (6)
O(32)	0.1047 (8)	0.3415 (10)	0.2878 (13)
O(33)	0.2349 (8)	0.4507 (9)	0.3483 (7)
O(34)	0.1255 (6)	0.4820 (7)	0.2918 (9)
OW1	0.2297 (6)	0.3928 (7)	0.0148 (8)
OW2	0.1749 (5)	0.2489 (6)	0.1638 (6)
N(1)	0.3154 (4)	0.3761 (4)	0.7029 (5)
N(2)	0.1629 (4)	0.4338 (4)	0.6786 (4)
N(1A)	0.4092 (4)	0.4719 (4)	0.5599 (5)
N(1B)	0.1909 (4)	0.3340 (4)	0.5503 (4)
C(1)	0.2750 (6)	0.3607 (6)	0.7959 (6)
C(2)	0.1697 (7)	0.3256 (6)	0.7962 (6)
C(3)	0.1468 (6)	0.4015 (7)	0.7750 (7)
C(1A)	0.4214 (6)	0.4172 (6)	0.7043 (6)
C(2A)	0.4615 (5)	0.4474 (5)	0.6125 (6)
C(3A)	0.5433 (5)	0.4542 (6)	0.5839 (6)
C(4A)	0.5774 (6)	0.4872 (6)	0.5023 (7)
C(5A)	0.5288 (6)	0.5143 (6)	0.4491 (7)
C(6A)	0.4413 (6)	0.5048 (6)	0.4787 (6)
C(1B)	0.0818 (6)	0.3740 (7)	0.6199 (7)
C(2B)	0.1007 (5)	0.3109 (5)	0.5618 (6)
C(3B)	0.0261 (6)	0.2301 (6)	0.5196 (7)
C(4B)	0.0538 (7)	0.1797 (7)	0.4630 (8)
C(5B)	0.1444 (6)	0.2060 (6)	0.4501 (7)
C(6B)	0.2125 (6)	0.2833 (6)	0.4958 (6)
H(O1)	0.2500	0.5195	0.4785
H(O2)	0.5625	0.3320	0.2500

The data were corrected for Lorentz-polarization effects, and an empirical absorption correction was applied. A total of 2747 independent data were collected, of which 1604 with $I > 1.5\sigma(I)$ were used in the analysis. Experimental parameters are collected in Table III.

Solution and Refinement of the Structure. In space group $P\bar{3}1c$ of the trigonal system with two molecules in the unit cell, the cobalt atom is constrained to lie on a crystallographic 3-fold axis. The positions of the unique cobalt and chromium atoms, the bridging oxygen atoms, and most of the ligand and anion atoms were found by direct methods with MULTAN.[14] Hydrogen atoms on the hydroxo groups were located in a dif-

(11) Figgis, B. N.; Nyholm, R. S. *J. Chem. Soc.* **1958**, 4190.
(12) Josephsen, J.; Pedersen, E. *Inorg. Chem.* **1977**, *16*, 2534.
(13) Pedersen, E. *Acta Chem. Scand.* **1972**, *26*, 333.

Table V. Absorption and Diffuse Reflectance Spectra of Compounds of the General Formula $[M^{II}\{(OH)_2CrA_4\}_3](ClO_4)_5 \cdot 6H_2O$[a]

		DMF		MF		CH_3CN		reflectance	
M(II)	A_4	λ_1, ϵ_1	λ_2, ϵ_2	λ_1, ϵ_1	λ_1, ϵ_1	λ_1, ϵ_1	λ_2, ϵ_2	λ_1	λ_2
Mg	bispictn	519, 246				516, 241	365, 275	516	368
Mn		517, 256				511, 275	409 sh, 269	515	380–400 sh
Co		516, 272				514, 264	340 sh, 284	516	380 sh
Ni		514.5, 258				510.5, 251	366, 253	512	384
Zn		513, 255	370, 295			511, 243	369, 260	513	372
Mg	4 × NH_3	516.5, 156	390, 137						
Mn		515.5, 181	380, 216						
Co		515, 179	389, 162						
Ni		510, 160	388, 144						
Zn		516, 157	389, 134						
Co	2 × en			494, 361	372, 331				
Ni				496, 298	375, 201				
Zn		511, 298	379, 222	495, 315	375, 182				
$[Cr(bispictn)(OH)(H_2O)](ClO_4)_2 \cdot 2H_2O$		519, 74.9	397, 71.3						
$[Cr(NH_3)_4(OH)(H_2O)](ClO_4)_2$		518.5, 54.8	399, 47.4						

[a] λ values in nm, and ε values in l mol^{-1} cm^{-1}. [b] Solvents: DMF = *N*,*N*′-dimethylformamide; MF = *N*-methylformamide.

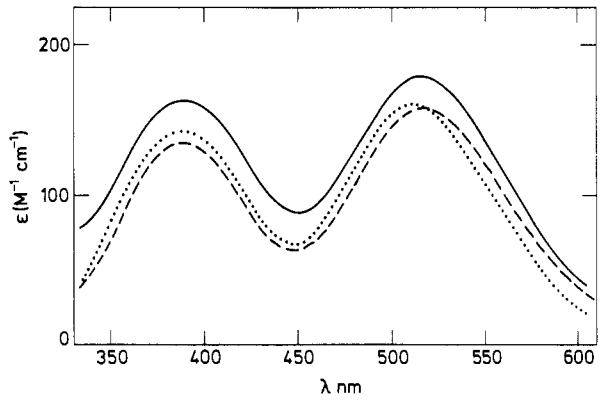

Figure 1. Absorption spectra (visible region) in DMF of $[Co\{(OH)_2Cr(NH_3)_4\}_3](ClO_4)_5 \cdot 6H_2O$ (solid line), $[Ni\{(OH)_2Cr(NH_3)_4\}_3](ClO_4)_5 \cdot 6H_2O$ (dotted line), and $[Zn\{(OH)_2Cr(NH_3)_4\}_3](ClO_4)_5 \cdot 4H_2O$ (dashed line).

ference Fourier map, ligand hydrogen atoms were placed in calculated positions, and water hydrogen atoms were not located; hydrogen atom coordinates were not refined, while all other atoms were refined anisotropically. The final values of the agreement factors were $R = 0.063$ and $R_w = 0.046$. The final values of the atomic coordinates, along with their standard deviations as estimated from the inverse matrix, are presented in Table IV. Hydrogen atom parameters, anisotropic thermal parameters, and observed and calculated structure amplitudes are available as supplementary material.

Results and Discussion

Synthesis. We have found that complexes containing tetranuclear ions of the general formulas $[M\{(OH)_2CrA_4\}_3]^{5+}$ and $[M\{(OH)_2CoA_4\}_3]^{5+}$ (where M = Mg, Mn, Co, Ni, and Zn and A_4 represents one tetradentate, two bidentate, or four monodentate amine ligands) are prepared simply by mixing aqueous solutions containing stoichiometric amounts of the divalent metal ions and of the "ligands", respectively. The ligand solutions contain the novel, positively charged bidentate ligands $[CrA_4(OH)_2]^+$ and their cobalt(III) analogue and are obtained by dissolving the corresponding hydroxo aqua complexes in water and adjusting the pH to ~8.5 with sodium hydroxide. As the amine ligands surrounding the Cr(III) and Co(III) centers, we have chosen the tetradentate ligand *N*,*N*′-bis(2-pyridylmethyl)-1,3-propanediamine (bispictn), the bidentate ligand 1,2-ethanediamine (en), and the monodentate ligand ammonia, but other amines work equally well.

The complexes described here are mostly isolated as perchlorate salts, and in all cases we isolated tetranuclear complexes. In a forthcoming publication, we will demonstrate the formation of related series of trinuclear complexes.[4]

Table VI. Interatomic Distances (Å) in $[Co\{(OH)_2Cr(bispictn)\}_3](ClO_4)_5 \cdot 6H_2O$

Co–O(1)	2.050 (5)	Co–O(2)	2.166 (5)
Cr–O(1)	1.902 (5)	Cr–O(2)	1.921 (5)
Cr–N(1)	2.068 (7)	Cr–N(1A)	2.063 (7)
Cr–N(1B)	2.085 (7)	Cr–N(2)	2.058 (7)
N(1)–C(1A)	1.494 (11)	N(2)–C(1B)	1.472 (11)
N(1A)–C(2A)	1.355 (10)	N(1B)–C(2B)	1.321 (10)
N(1A)–C(6A)	1.333 (11)	N(1B)–C(6B)	1.326 (10)
C(2A)–C(1A)	1.505 (12)	C(2B)–C(1B)	1.486 (12)
C(2A)–C(3A)	1.340 (11)	C(2B)–C(3B)	1.410 (12)
C(3A)–C(4A)	1.345 (13)	C(3B)–C(4B)	1.398 (14)
C(4A)–C(5A)	1.340 (14)	C(4B)–C(5B)	1.318 (13)
C(5A)–C(6A)	1.414 (11)	C(5B)–C(6B)	1.368 (12)
N(1)–C(1)	1.514 (10)	N(2)–C(3)	1.524 (11)
C(1)–C(2)	1.499 (12)	Co–Cr	3.064 (11)

Table VII. Selected Interatomic Angles (deg) in $[Co\{(OH)_2Cr(bispictn)\}_3](ClO_4)_5 \cdot 6H_2O$

O(1)–Co–O(2)	75.6 (2)	O(1)–Co–O(1′)	99.1 (2)
O(1)–Co–O(2′)	164.9 (2)	O(1)–Co–O(2″)	95.7 (2)
O(1)–Cr–O(2)	85.2 (2)	O(1)–Cr–N(1)	176.4 (2)
O(1)–Cr–N(2)	87.8 (2)	O(1)–Cr–N(1A)	96.9 (2)
O(1)–Cr–N(1B)	92.6 (2)	O(2)–Cr–N(1)	93.8 (2)
O(2)–Cr–N(2)	92.8 (2)	O(2)–Cr–N(1A)	89.8 (2)
O(2)–Cr–N(1B)	173.7 (2)	N(1)–Cr–N(2)	95.7 (2)
N(1)–Cr–N(1A)	79.6 (2)	N(1)–Cr–N(1B)	88.8 (2)
N(2)–Cr–N(1A)	174.8 (2)	N(2)–Cr–N(1B)	81.2 (2)
N(1A)–Cr–N(1B)	96.3 (2)	N(1)–C(1)–C(2)	112.3 (7)
C(1)–C(2)–C(3)	113.0 (8)	N(2)–C(3)–C(2)	114.8 (7)
C(1)–N(1)–C(1A)	111.3 (6)	C(3)–N(2)–C(1B)	114.0 (7)
C(2A)–N(1A)–C(6A)	118.6 (7)	C(2B)–N(1B)–C(6B)	120.1 (7)
C(1A)–C(2A)–C(3A)	124.8 (8)	C(1B)–C(2B)–C(3B)	121.8 (8)
C(2A)–C(3A)–C(4A)	121.3 (9)	C(2B)–C(3B)–C(4B)	116.1 (9)
C(3A)–C(4A)–C(5A)	119.2 (9)	C(3B)–C(4B)–C(5B)	122.0 (9)
C(4A)–C(5A)–C(6A)	119.4 (9)	C(4B)–C(5B)–C(6B)	118.4 (9)

Electronic Spectra. Representative visible absorption spectra of the chromium complexes are presented in Figure 1 and in Table V. The choice of solvent was made in order to maximize the solubility of the complex. The spectra change very slowly with time; for comparison with the solution spectra, we have measured the diffuse reflectance spectra of the complexes with bispictn and find good agreement between solution and solid-state spectra.

The spectra are dominated by the two spin-allowed chromium(III) bands at approximately 510–519 and 365–390 nm. The spectra resemble those of the parent aqua hydroxo complexes, which is consistent with the presence of the hydroxo bridges in the complexes.

Description of the Structure. The structure consists of $[Co\{(OH)_2Cr(bispictn)\}_3]^{5+}$ cations, perchlorate anions, and water

(14) Germain, G.; Main, P.; Woolfson, M. M. *Acta Crystallogr., Sect. A* **1971**, *A27*, 368.

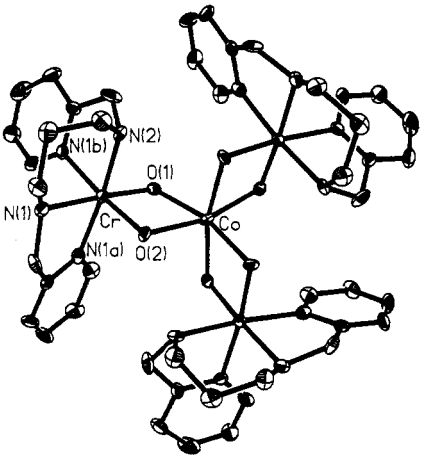

Figure 2. View of the entire $[Co\{(OH)_2Cr(bispictn)\}_3]^{5+}$ cation in the crystals of $[Co\{(OH)_2Cr(bispictn)\}_3](ClO_4)_5 \cdot 6H_2O$. Hydrogen atoms are omitted for clarity. Carbon atoms have not been labeled, but the numbering scheme for the pyridine rings follows standard practice. Unlabeled nitrogen atoms are related to labeled atoms by the 3-fold axis through Co.

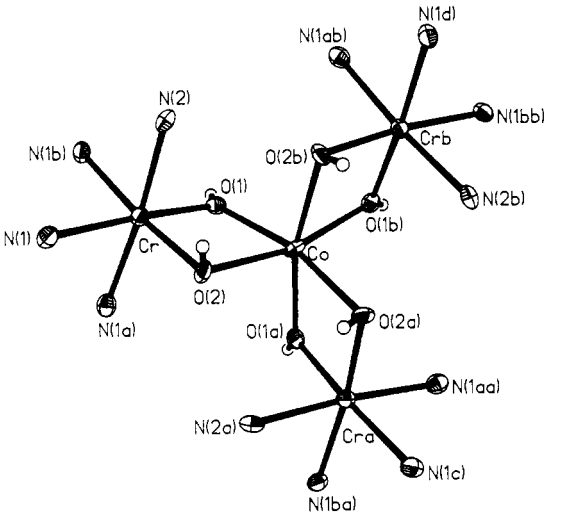

Figure 3. Inner coordination spheres around the cobalt and chromium atoms in the $[Co\{(OH)_2Cr(bispictn)\}_3]^{5+}$ cation. Hydrogen atoms are shown as spheres of arbitrary size. Atoms N(1c) and N(1d) are related by the 3-fold axis to atom N(1), as are atoms N(2a) and N(2b) to N(2); all of these atoms are amine nitrogen atoms, while other nitrogen atoms are pyridine nitrogen atoms.

molecules. A view of the entire complex cation is given in Figure 2, and the inner coordination spheres around the metal centers are depicted in Figure 3. The principal bond lengths and angles in the complex cation are listed in Tables VI and VII, respectively.

The complex cation has crystallographically imposed C_3 symmetry. The Co atom lies on the 3-fold axis and is surrounded by the six bridging hydroxo groups, which serve as pairwise bridges to the three chromium(III) centers. Alternatively, and probably more appropriately, the complex can be viewed as consisting of three *cis*-$[Cr(bispictn)(OH)_2]^+$ units, which act as bidentate ligands to the central cobalt(II) core. As can be seen in Figure 2, the configuration at both the cobalt and chromium centers is Λ. Naturally, since we used the β isomer of the chromium(III) starting material, the isomer isolated here is again the β form in which the two pyridine nitrogen atoms are cis to each other. As can also be deduced from an examination of Figure 2, the absolute configurations at both amine nitrogen atoms [N(1) and N(2)] is *R*; hence, the geometries at the three chromium centers can best be described as $\Lambda(\beta)RR'\Lambda(\beta)RR'\Lambda(\beta)RR'$. The geometry of Co, which is rigorously C_3, only poorly approximates octahedral. The Co–O bond lengths of 2.050 (5) and 2.166 (5) Å differ significantly, and the O(1)–Co–O(2) angle subtended by the bidentate unit is only 75.6 (2)°. The geometry at chromium is also distorted from octahedral, the cis bond angles lying in the range 79.7 (3)–96.9 (3)°, while trans angles are from 173.7 (3) to 176.4 (3)°. The O(1)–Cr–O(2) angle is 85.2 (2)°. The four Cr–N distances fall in the range 2.058 (7)–2.085 (7) Å [average value 2.067 (12) Å], with no discernible difference between the Cr–N(pyridine) and Cr–N(amine) distances, while the Cr–O distances are 1.902 (5) and 1.921 (5) Å. The bridging Cr–O–Co angles are asymmetric, the Cr–O(1)–Co angle of 101.6 (2)° being significantly larger than the value of 96.9 (2)° at O(2); both of these values are within the range normally observed for M–O–M angles in binuclear bis(μ-hydroxo)[15,16] and bis(μ-oxo)[17] transition-metal complexes. The Co–Cr distance in the tetramer is 3.064 (2) Å, comparable to the values in bis(μ-hydroxo)dichromium(III) dimers.[15] Unlike these binuclear systems, however, the bridging Cr–O(1)–Co–O(2) unit is not planar, the cobalt and chromium atoms lying 0.047 and 0.056 (2) Å, respectively, below the least-squares plane, while the oxygen atoms O(1) and O(2) lie 0.053 (6) and 0.049 (6) Å, respectively, above it.

The ligand geometries are unremarkable and are comparable with those reported for other complexes or bispictn and its analogues.[17-20] Thus, the pyridine rings are planar, with no atom deviating from the least-squares plane by more than 0.017 (9) Å. The nominally tetrahedral angles at amine nitrogen atoms are slightly enlarged, the values of the C–N–C angles being 111.3 (6) and 114.0 (7)° at N(1) and N(2), respectively. The two five-membered chelate rings are both in the envelope conformation; in one case, the four atoms Cr, N(1A), C(2A), and C(1A) are approximately planar (average deviation 0.006 Å) and the pyridine nitrogen atom N(1) lies 0.625 Å below the plane, while in the other the analogous four atoms Cr, N(1B), C(2B), and C(1B) are coplanar (maximum deviation 0.004 Å), while pyridine nitrogen atom N(2) lies 0.466 Å above the plane. The six-membered chelate ring forms an almost idealized flattened chair. In the chair conformation, the three atoms N(1), N(2), and C(2) lie in a plane that is parallel to the plane formed by the other three atoms Cr, C(1), and C(3). In the flattened chair, Cr has rotated about the N(1)–N(2) axis so that it now lies in the plane N(1), N(2), and C(2), the average deviation from the four-atom plane being 0.006 Å, while C(1) and C(3) lie 0.587 and 0.507 Å, respectively, above the plane. In the familiar cyclohexane structure, therefore, the present conformation would correspond to the situation where atoms C(1), C(2), C(4), and C(6) were coplanar while C(3) and C(5) are both on the same side of the plane. The flattening can also be described by the small values of the torsion angles around the Cr–N(2) and Cr–N(1) bonds, which are 21.4 and −25.2°, respectively.

There are three crystallographically independent perchlorate ions. Atoms Cl(1) and Cl(2) lie on 3-fold axes, which also pass through one oxygen atom of each anion [O(11) and O(21), respectively]. These two anions, therefore, exhibit idealized C_3 symmetry, but each approximates tetrahedral geometry; at Cl(1), the Cl–O bond lengths are 1.402 (12) and 1.389 (7) Å and the O–Cl–O angles are 109.5 (4)°, while at Cl(2) the distortion is slightly greater, with Cl–O bond lengths of 1.22 (3) and 1.310 (2) Å and associated O–Cl–O angles of 106.9 (8)°. The third chlorine atom, Cl(3), is in a general position and exhibits bond lengths and angles in the ranges 1.276 (10)–1.415 (15) Å and 104.0 (10)–118.7 (10)°.

Parametrization of Susceptibility Data. The magnetic susceptibilities of the four compounds based on the $MnCr_3$, $NiCr_3$, and $ZnCr_3$ units all showed increasing susceptibilities with de-

(15) Hodgson, D. J. In *Magneto-Structural Correlations in Exchange Coupled Systems*; Willett, R. D., Gatteschi, D., Kahn, O., Eds.; Reidel: Dordrecht, The Netherlands, 1985; pp 497–592.
(16) Hodgson, D. J. *J. Mol. Catal.* **1984**, *23*, 219 and references therein.
(17) See, for example: Goodson, P. A.; Glerup, J.; Hodgson, D. J.; Michelsen, K.; Pedersen, E. *Inorg. Chem.* **1990**, *29*, 503–508.
(18) Goodson, P. A.; Hodgson, D. J. *Inorg. Chem.* **1989**, *28*, 3606–3608.
(19) Goodson, P. A.; Oki, A. R.; Glerup, J.; Hodgson, D. J. *J. Am. Chem. Soc.*, in press.
(20) Fischer, H. R.; Hodgson, D. J.; Michelsen, K.; Pedersen, E. *Inorg. Chim. Acta* **1984**, *88*, 143–150.

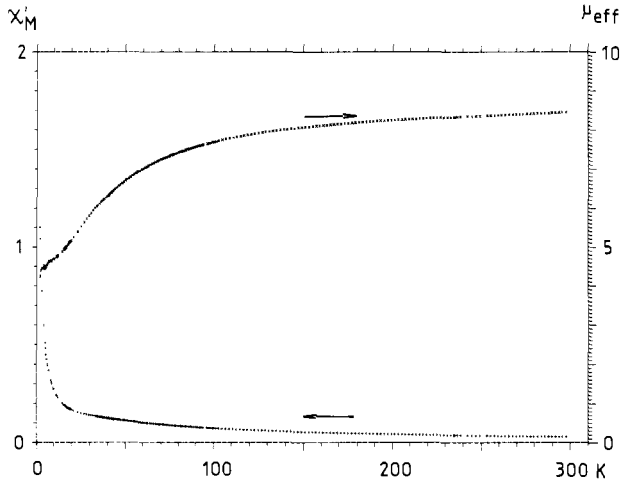

Figure 4. Magnetic properites of $[Mn\{(OH)_2Cr(bispictn)\}_3](ClO_4)_5 \cdot 6H_2O$: susceptibility (left scale) in cgs units per formula unit, and effective magnetic moment (right scale) in Bohr magnetons. Magnetic field = 13 000 G.

creasing temperature down to 2 K, which is our lower limit. The effective magnetic moments were decreasing in characteristic ways with decreasing temperature. As an example, the data for the $MnCr_3$ complex are shown in Figure 4. The susceptibilities were interpreted in terms of diagonalization of the isotropic Heisenberg-type Hamiltonian

$$\hat{H} = \sum_{k<l}\{J_{kl}\hat{S}_k \cdot \hat{S}_l + j_{kl}(\hat{S}_k \cdot \hat{S}_l)^2\} + \beta g\hat{H} \cdot \hat{S} \qquad (1)$$

For Cr(III), Mn(II), Ni(II), and Zn(II) the obvious choice of spin values were $^3/_2$, $^5/_2$, 1, and 0, respectively. For Co(II) we decided to choose a value of $^3/_2$, since our calculations did not allow nonzero angular momenta.

The data were fitted to the expression

$$\chi'_{mol} = -\frac{N}{H}\frac{\sum_i \frac{\delta E_i}{\delta H}\exp(-E_i/kT)}{\sum_i \exp(-E_i/kT)} + K + \frac{C}{T} \qquad (2)$$

by minimization of

$$\sum_j \frac{[\chi_{obsd}(T_j) - \chi'(T_j)]^2}{\sigma^2(\chi(T_j)) + \left(\frac{\delta\chi_{obsd}}{\delta T}(T_j)\right)^2 \sigma^2(T_j)} \qquad (3)$$

Here χ_{obsd} is the measured molar susceptibility, corrected for diamagnetic contributions by using the Pascal constants. E_i values are the energies of the components of the ground-state manifold. The adjustable parameters are J_{kl} and g. It was in no case possible to get reliable fits if biquadratic terms, j_{kl}, a Curie term, C, or an additive constant, K, were included. The computer programs have been described earlier.[21] With use of eq 2 in the calculation of $\chi'(I)$, saturation effects at 13 kG and low temperature are included. These effects can be very important in these systems where the ground states may acquire spin values of $S \leq 7$.

The results of the data fittings are shown in Table VIII. General energy diagrams illustrating the relation among energy, spin, and degeneracy for tetranuclear systems having S_1 between $^1/_2$ and $^5/_2$, $S_2 = S_3 = S_4 = {}^3/_2$, $J_{12} = J_{13} = J_{14} = J$, and $J_{23} = J_{34} = J_{42} = 0$ are shown in Figure 5a–e. Taking the system with $S_1 = {}^1/_2$ as an example (Figure 5a), we see that for an antiferromagnetically coupled system ($J > 0$) the ground state is a nonet ($S = S_1 + S_2 + S_3 + S_4 = 4$) and that the nearest excited states are two degenerate septets at an energy of $J/2$. Then the spins increase again and, finally, an undecet ($S = 5$) is the state of highest energy, $5J$, among the coupled ground states. For a ferromagnetically coupled system ($J < 0$) this undecet is the ground state, and the state with highest energy is the nonet at $-5J$.

For the other systems with $S_1 > {}^1/_2$ related behavior is observed. The states are clearly grouped in families, and in every case, independent of S_1 and the sign of J, the ground state has a higher spin than the nearest excited states. This has peculiar consequences for the variation of the effective magnetic moments with the temperature. The low-temperature limits of these moments at zero magnetic field are given in Table IX. The variations with temperature are illustated in Figure 6, calculated on the assumptions $g = 2$ and $H = 13\,000$ G. In the range $|kT/J| < 1$, saturation effects are important. For small values of H all antiferromagnetically coupled systems exhibit a minimum value of μ_{eff}. Figure 6 might leave the impression that the antiferromagnetic systems all have the same values of μ_{eff} at 57 K, but this is only approximately true, of course. For nonzero values of H all ferromagnetic systems show maxima of μ_{eff} vs T. If the corners in these "magnetic triangles" are allowed to interact, the degeneracies shown in Figure 5 partly disappear.

Discussion of the Magnetic Parameters. The MCr_3 clusters with M = Mn(II), Ni(II), and Co(II) all show antiferromagnetic exchange of the order of $J_{MCr} \leq 5$ cm^{-1}, referring to the Hamiltonian eq 1. For M = Zn(II) this value is, of course, zero. For M = Mn(II), Ni(II), and Zn(II), $J_{CrCr} \sim 1$ cm^{-1}. For M = Co(II), the coupling was very small, and J_{CrCr} and J_{CoCr} could not be determined independently. A correlation coefficient of −0.9992 was found. The result of a two-parameter fitting is shown

Table VIII. Parameters Obtained from Magnetic Susceptibilities

unit	parameters	calcd energies E_i, cm^{-1}	spin
$MnCr_3$	$J_{MnCr} = 5.61$ (2) cm^{-1}	0.00	2
		10.60	1
	$J_{CrCr} = 0.76$ (4) cm^{-1}	10.60	1
		16.82	3
	$g = 1.980$ (1)	21.82	2
		21.82	2
	var/f = 1.07	21.97	0
$CoCr_3$	$J_{CoCr} = 1.01$ (5) cm^{-1}	0.00	3
		1.76	2
	J_{CrCr} set to zero	1.76	2
		3.52	1
	$g = 2.175$ (2)	3.52	1
		3.52	1
	var/f = 3.65	4.69	4
$NiCr_3$	$J_{NiCr} = 4.87$ (6) cm^{-1}	0.00	3.5
		0.10	2.5
	$J_{CrCr} = 1.06$ (1) cm^{-1}	0.10	2.5
		1.26	1.5
	$g = 1.993$ (1)	1.26	1.5
		1.26	1.5
	var/f = 1.11	3.49	0.5
$ZnCr_3$	$J_{CrCr} = 1.06$ (1) cm^{-1}	0.00	0.5
		0.00	0.5
	$g = 1.972$ (2)	1.60	1.5
		1.60	1.5
	var/f = 4.9	1.60	1.5
		1.60	1.5
		4.26	2.5

Table IX. Ground-State Magnetism at Zero Field and Temperature

S_1[a]	S for $J > 0$	μ_{eff}	S for $J < 0$	μ_{eff}
$^5/_2$	2	$\sqrt{24} = 4.90$	7	$\sqrt{224} = 14.97$
2	$^5/_2$	$\sqrt{35} = 5.92$	$^{13}/_2$	$\sqrt{195} = 13.96$
$^3/_2$	3	$\sqrt{48} = 6.93$	6	$\sqrt{168} = 12.96$
1	$^7/_2$	$\sqrt{63} = 7.94$	$^{11}/_2$	$\sqrt{143} = 11.96$
$^1/_2$	4	$\sqrt{80} = 8.94$	5	$\sqrt{120} = 10.95$

[a] S_1 refers to a spin interacting with three equivalent spins of $^3/_2$.

(21) Andersen, P.; Damhus, T.; Pedersen, E.; Petersen, A. *Acta Chem. Scand., Ser. A* **1984**, *A38*, 359.

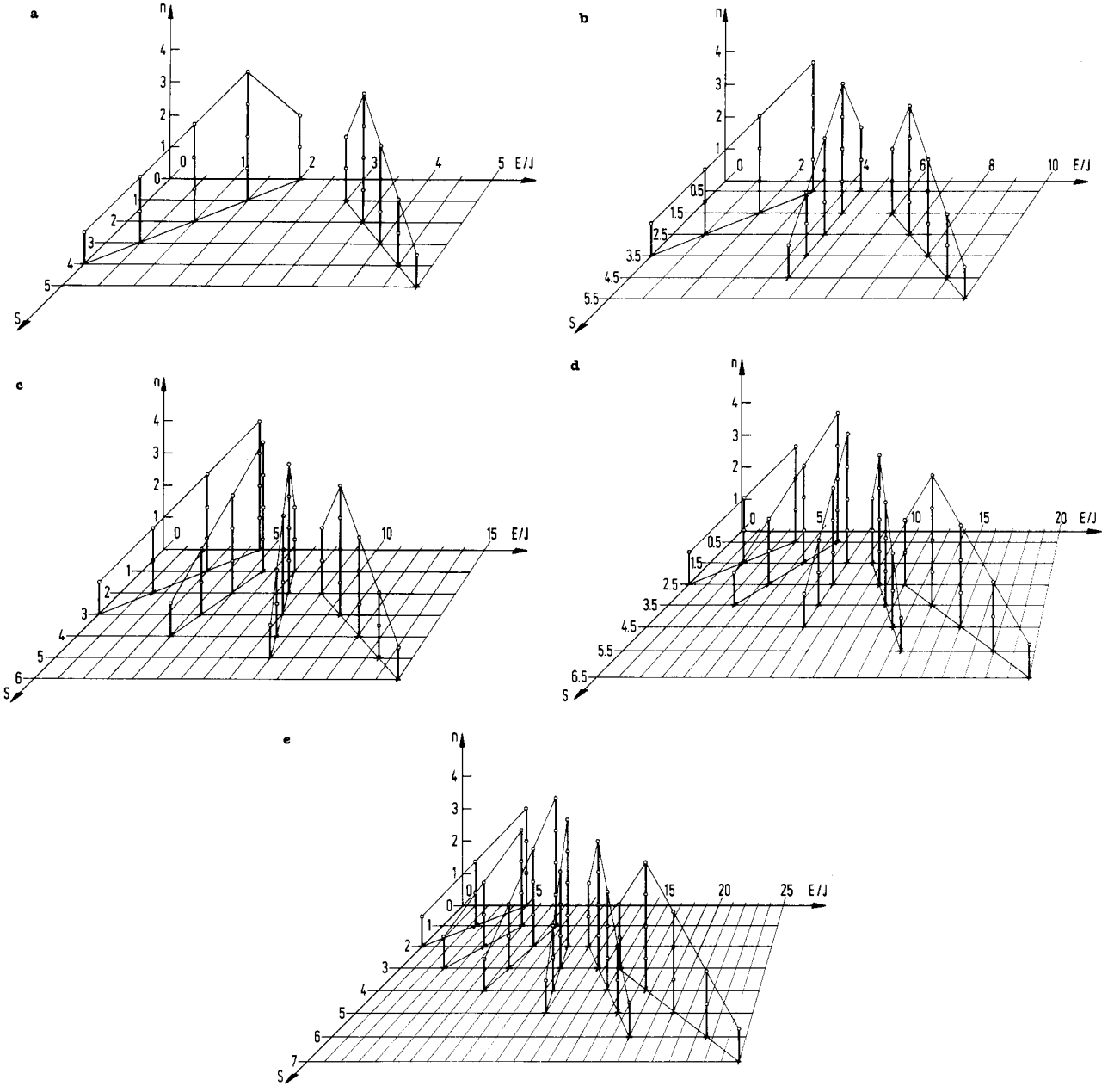

Figure 5. Energy diagrams, showing energies (units of J), total spin values S, and degeneracy n for three equivalent spins of $^3/_2$, each of which is coupled to S_1. For antiferromagnetic ground states ($J > 0$), the far left state is the ground state; for ferromagnetic ground states ($J < 0$), the far right state is the ground state. Key: (a) $S_1 = {}^1/_2$; (b) $S_1 = 1$; (c) $S_1 = {}^3/_2$; (d) $S_1 = 2$; (e) $S_1 = {}^5/_2$.

in Table VIII. A g value in excess of 2 reflects the orbital contribution to the magnetism of Co(II).

The coupling parameters in Table VIII are all positive, corresponding to antiferromagnetic exchange in our notation (eq 1). Recently, a material has been prepared[22] by coprecipitation of "$[Ni(Me_6\text{-}[14]ane\text{-}N_4)]^{2+}$" and $[Cr(ox)_3]^{3-}$ (molar ratio 3:1) in the presence of perchlorate ions. This material has not been structurally characterized but is referred to[22] as a $Cr^{III}Ni^{II}_3$ complex, magnetically related to the present series of complexes. The magnetism of the $CrNi_3$ material was interpreted in terms of ferromagnetic interactions between Cr(III) and Ni(II), giving $J_{CrNi} = -5.3$ cm^{-1} in our notation. This value is numerically surprisingly large considering the metal-to-metal distance in the postulated CrC_2O_4Ni fragment.

The coupling parameters in Table VIII should also be compared with the results for a structurally related system[21] based on $Cr_a^{III}Cr_b^{III}{}_3$ units, where $J_{Cr_aCr_b} \sim 11$ cm^{-1} and $J_{Cr_bCr_b} \sim 1$ cm^{-1}. The GHP model[23] provides a route for such a comparison. In the $M^{III}Cr_3$ series all interactions are expected to be numerically larger than observed for the $M^{II}Cr_3$ series due to their shorter metal-to-metal distances. For all the systems it is true, however, that the orbital-overlap contribution to the magnetic coupling is a sum of several competing antiferro- and ferromagnetic terms besides the small ferromagnetic term always present. In the heteronuclear systems, calculations are further complicated by the fact that the energies of the charge-transfer states depend on the direction of the electron transfer. This will be the subject of a future publication.

EPR Spectra. Solid-state EPR spectra of all the present complexes contain only broad peaks centered at $g \sim 2$ at X-band frequencies even when measured at 3 K. This is not surprising, since the complexes are magnetically concentrated and since cooling leads to population of high-spin ground states.

It was attempted to precipitate solid solutions containing <1 mol % of the MCr_3 complexes in the isomorphous and diamagnetic

(22) Pei, Y.; Journaux, Y.; Kahn, O. *Inorg. Chem.* **1989**, *28*, 100.

(23) Glerup, J.; Hodgson, D. J.; Pedersen, E. *Acta Chem. Scand., Ser. A* **1983**, *A37*, 161.

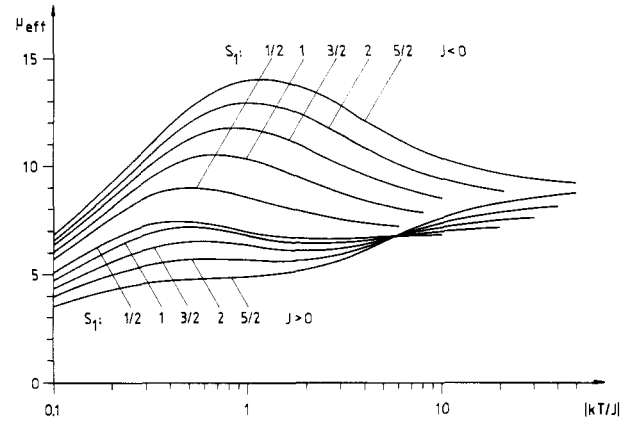

Figure 6. Effective magnetic moments (Bohr magnetons) of systems with three equivalent spins of $^3/_2$, each of which is coupled to S_1. $g = 2$, and magnetic field = 13 000 G. J is defined as in eq 1; $J < 0$ corresponds to ferromagnetic coupling.

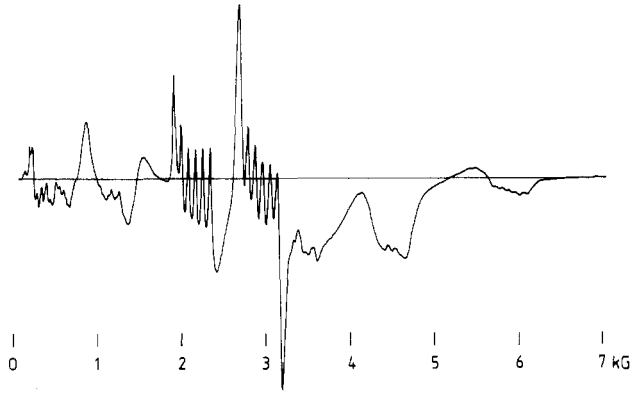

Figure 7. EPR spectrum (first derivative) of 1% Mn^{2+} in $[Zn\{(OH)_2Co(bispictn)\}_3](ClO_4)_5 \cdot 5H_2O$ at 9.38 GHz and 4 K.

$ZnCo^{III}_3$ systems. We obtained a lot of ornamental EPR spectra, the reason being the lability of the MM'_3 units even in nonaqueous solutions. The concentrations of the desired species are extremely small after complete scrambling, and the EPR spectra were dominated by other species as $M^{II}Co^{III}_3$ and $M^{II}Cr^{III}Co^{III}_2$, for example.

In Figure 7 is shown the EPR spectrum of the $MnCo_3$ complex diluted in the isomorphous and diamagnetic host $[Zn\{(OH)_2Co(bispictn)\}_3](ClO_4)_5 \cdot 6H_2O$. This spectrum is typical of an axially distorted Mn^{2+} ion with $S = {}^5/_2$ and $I = {}^5/_2$. Easily identifiable hyperfine multiplets are centered around approximately 5900, 4500, 2900, and 2100 G. These signals from the randomly oriented powder sample have their main contributions from molecular orientations having β values of 90 and 10.5°, 68 and 35°, 70–90°, and 90 and 55°, respectively. Here β refers to the angle between the field and the molecular symmetry axis (3-fold or higher). This interpretation corresponds to the spin Hamiltonian parameters $|D| = 0.11\ cm^{-1}$, $g = 2.00$, $A_\parallel = 75 \times 10^{-4}\ cm^{-1}$, and $|A_\perp| = 83 \times 10^{-4}\ cm^{-1}$ for a system with $S = I = {}^5/_2$. These results are typical for Mn^{2+} in a distorted octahedral coordination to oxygen ligators. These parameters were obtained by a simulation procedure. Previously, a diagram showing the parallel and perpendicular resonant field positions at which $\Delta M_s = \pm 1$ transitions occur as functions of the zero-field-splitting parameter D has been published.[24] This diagram may be misleading in this case where intermediate orientations are very important.

Acknowledgment. This work was supported by the National Science Foundation through Grant Nos. CHE-9007607 and CHE-8912675 (to D.J.H.), by the Danish National Science Research Council through Grant No. 511-5680 (to E.P.), and by the Scientific Affairs Division, North Atlantic Treaty Organization (NATO), through Grant No. 85/0790 (to D.J.H., K.M., and E.P.). We are very grateful to Ms. Solveig Kallesøe and Ms. Karen Magrethe Nielsen for experimental assistance.

Supplementary Material Available: For $[Co\{(OH)_2Cr(bispictn)\}_3](ClO_4)_5 \cdot 6H_2O$, Tables S1 (hydrogen atom parameters) and S2 (anisotropic thermal parameters) (3 pages); Table S3 (observed and calculated structure amplitudes) (12 pages). Ordering information is given on any current masthead page.

(24) DeVore, T. C.; Van Zee, R. J.; Weltner, W., Jr. *J. Chem. Phys.* **1978**, *68*, 3522.